

Studies of MeV Fast Protons Produced in Laser Fusion Experiments

D. G. Hicks, C. K. Li, F. H. Séguin, A. K. Ram, and R. D. Petrasso

Plasma Science and Fusion Center, Massachusetts Institute of Technology, Massachusetts 02139

J. M. Soures, D. D. Meyerhofer, S. Roberts, J. D. Schnittman, C. Sorce, and C. Stöckl

Laboratory for Laser Energetics, University of Rochester, Rochester, New York 14623

T. C. Sangster and T. W. Phillips

Lawrence Livermore National Laboratory, Livermore, California 94550

(November 24, 1999)

Enhanced laser-induced acceleration of fast protons up to $\gtrsim 1$ MeV has been observed on the 60-beam, 30-kJ OMEGA laser at intensities of 10^{15} Wcm $^{-2}$. These energies are more than 5 times greater than previously observed on single-beam experiments at equivalent intensities. The total energy in these protons is $\sim 0.1\%$ of the laser energy and inferred hot electron temperatures are 10 – 20 keV. High-resolution spectroscopy has detected proton spectra with intense, regular lines.

A number of experiments have observed that ions at suprathermal energies are produced during high-intensity laser interactions with solids [1] – [6]. These experiments show that protons are always present in the ion signal, regardless of the type of target material. Such accelerated ions, or fast ions, are thought to be associated with hot electrons [7] – [9] which produce electrostatic fields through charge separation.

A distinctive feature of fast proton spectra is the presence of a well-defined, maximum cutoff energy. For single-beam experiments, Tan et al. [1] observed the scaling of maximum proton energy with laser intensity to be:

$$E_{\max} = 3.51 \times 10^{-3} (I\lambda^2)^{1/3} \quad (1)$$

over the range $I\lambda^2 = 10^{14} - 3 \times 10^{18}$ Wcm $^{-2}\mu\text{m}^2$, where E_{\max} is the maximum proton energy in keV, I is the laser intensity in Wcm $^{-2}$, and λ is the laser wavelength in μm . More recently, this relationship has been verified at high intensities with substantially different laser conditions [2,6]. At least 3 different detector types were used in all these studies. From this scaling, it would be expected that, at $I\lambda^2 = 10^{14}$ Wcm $^{-2}\mu\text{m}^2$ corresponding to conditions on laser fusion experiments, $E_{\max} \sim 160$ keV. Instead, our studies on the 60-beam OMEGA laser have measured proton energies greater than 1 MeV. In addition to observing these unexpectedly high maximum energies, we have also performed high-resolution measurements of the proton spectra. Previous studies of the proton spectrum using low-resolution time-of-flight techniques often showed exponential-like velocity spectra consistent with the isothermal, self-similar plasma-

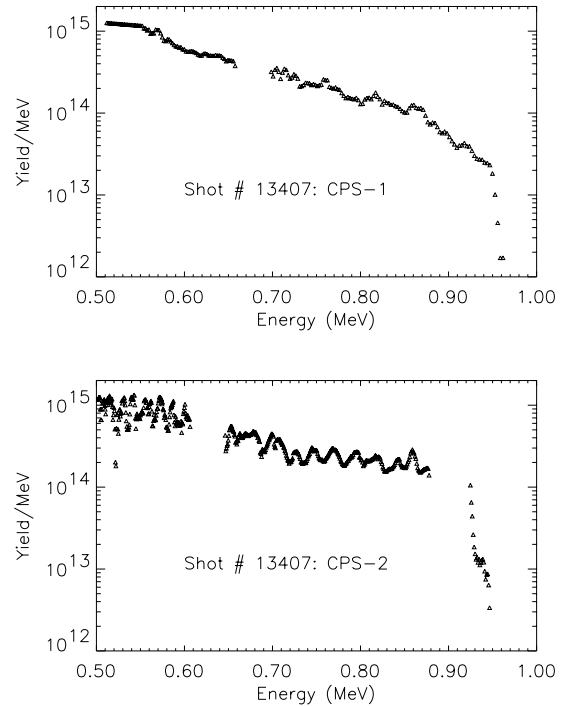


FIG. 1. Fast proton spectra for a single shot measured concurrently by the two spectrometers, CPS-1 (at 235 cm) and CPS-2 (at 100 cm). The gaps are due to detector dead space. Total particle yield per MeV is inferred by assuming isotropic emission over all solid angles. Although the spectral shapes differ, the endpoint energies are approximately equal.

expansion model [1,11] or its modifications which include two electron temperatures [8] or multi-ion species [4,5]. Our high-resolution studies reveal for the first time the presence of intense, regular spectral lines.

The experiments were performed on the OMEGA laser system at the Laboratory for Laser Energetics, University of Rochester. OMEGA is a 60-beam, neodymium-doped phosphate glass laser capable of delivering 30 kJ of frequency-tripled, $0.35 \mu\text{m}$ light [12]. Irradiation uniformity is accomplished using distributed phase plates and smoothing by spectral dispersion (SSD) [13]. For these studies, laser pulse shapes were mostly 1-ns square, with a few 400-ps square pulses. The laser, which was used to

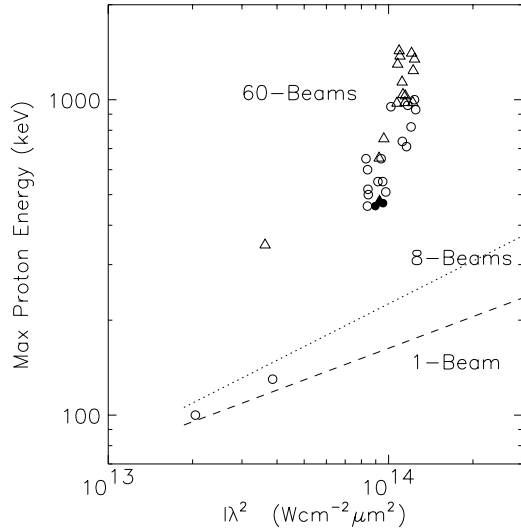


FIG. 2. Scaling of maximum fast-proton energy with $I\lambda^2$: open and solid circles are for glass targets with 1 ns and 0.4 ns pulses respectively, while open and solid triangles are for plastic targets with 1 ns and 0.4 ns pulses respectively. Error bars, at less than 2 %, are smaller than the plotting symbols. The dashed line is extrapolated from the scaling of single-beam experiments (Eq. 1), while the dotted line is from experiments using 8-beams [1]. There is no significant difference between shots with or without SSD.

directly illuminate the target, delivered energies of 10 to 30 kJ. Laser intensities varied from 10^{14} to 10^{15} Wcm^{-2} , where the intensity is calculated by dividing total incident laser energy by pulse length and target surface area. Targets were 0.9 – 1 mm diameter spherical microballons with glass or paralene (CH) shell material ranging from 2 to 20 μm in thickness.

Proton spectra were observed using a charged-particle spectrometer [14] consisting of a 7.6-kG permanent magnet with CR-39 nuclear track-etch detectors. The instrument can measure total particle yields between 10^7 and 10^{16} and proton energies from 0.1 to 40 MeV. Use of a high-field magnet in conjunction with single-particle discrimination from track detectors gives this instrument high energy resolution: better than 1 % over the energy range for fast ions, or $\lesssim 3$ keV at 500 keV. Systematic uncertainties are $< 2\%$. A rapid, automated scanning system was developed which can readily count 10^6 tracks per shot. Simultaneous measurements are made by two virtually identical spectrometers positioned 101° apart, one outside the OMEGA chamber at 235 cm from the target (CPS-1), the other inside at 100 cm (CPS-2).

Sample spectra obtained simultaneously by each spectrometer are illustrated in Fig. 1, clearly showing the characteristic maximum cutoff energy [15]. Despite different spectral shapes, the endpoint energies observed from both views are approximately equal and generally are within 50 keV of each other (where the systematic

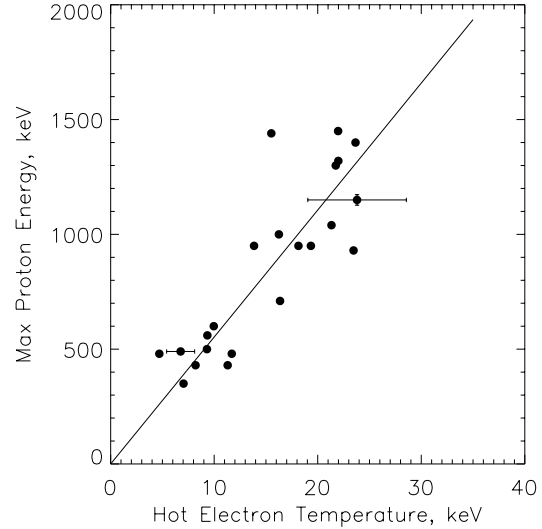


FIG. 3. Maximum proton energy versus the hot electron temperature inferred from the slope of the ion velocity spectrum. Uncertainties in the inferred temperature are caused by uncertainties in determining the spectral slope. The linear relation is in agreement with that found for single-beam experiments in Ref. [1].

error between instruments is < 40 keV).

The measurements of maximum proton energy are plotted versus $I\lambda^2$ in Fig. 2. The scaling found previously on single-beam and 8-beam experiments [1] are shown by the dashed and dotted lines respectively. For intensities less than $\sim 1.6 \times 10^{14}$ Wcm^{-2} , the proton energies are below the detectable limit of 100 keV, while at intensities of 10^{15} Wcm^{-2} energies up to 1.4 MeV were observed. Neither laser-pulse duration (at 0.4 or 1 ns) nor application of SSD appear to make any substantial difference to the maximum proton energies; however, as Fig. 2 shows, maximum energies are generally higher for CH targets than they are for glass targets.

As illustrated in Fig. 2, the measured proton energies of ~ 1 MeV are more than 5 times greater than those observed previously at the same $I\lambda^2$ [1]. In order to place the OMEGA measurements in context, it is useful to examine more closely some of these previous studies. The relationship given by Eq. 1 (dashed line in Fig. 2) was determined by studies over 4 orders of magnitude in intensity using nanosecond pulses of 10.6 μm light at energies up to 1 kJ focused to spot sizes of ~ 100 μm [1]. A similar scaling was found using picosecond pulses of 1.05 μm light at low energy (30 J) focused to spot sizes of ~ 12 μm [2]. Despite the substantially different laser conditions of these two studies, there was no indication of any significant deviation from the scaling given by Eq. 1, at least for the range of conditions covered by these single-beam experiments. On the other hand, for experiments using 8 beams, a stronger scaling with $I\lambda^2$

was observed (dotted line in Fig. 2) [1,10]. It is notable that these multi-beam experiments found that maximum proton energies were dependent on the target material whereas the single-beam experiments observed no such dependency. On the 60-beam OMEGA laser, we observe an even stronger scaling with $I\lambda^2$ than observed on the 8-beam studies and we find that glass and CH targets lead to different maximum proton energies. This evidence would appear to suggest that the presence of many beams on OMEGA might be the cause of these elevated proton energies. However, it should be emphasized that laser conditions on OMEGA are unique in many other ways besides the presence of 60 beams and, without performing a systematic study, it is difficult to isolate any single factor that might be responsible for producing the elevated proton energies.

Since fast ions are generally thought to be associated with hot electrons driving the plasma expansion into vacuum [7–9], it is useful to infer an effective hot electron temperature from the proton spectra. To do this requires that a model be used to describe the plasma expansion. One such description is the isothermal, self-similar model [7] which predicts that the slope of the velocity spectrum is a function of the hot electron temperature, T_h . For our studies, the spectra do not always have a single, well-defined slope; however their character is generally exponential-like and by a least-squares fit to the velocity spectra (avoiding the steep endpoint region), the average slope and thus an effective temperature can be determined. In Fig. 3 it is shown that the maximum proton energy is proportional to the inferred T_h , with a best fit giving the relationship $E_{\max}/T_h = 55$. This value is close to that found experimentally by Tan et al. [1] where $E_{\max}/T_h = 66$, though, to the best of our knowledge, there is no theoretical explanation for this constant ratio. We thus infer that the elevated proton energies are driven by effective hot electron temperatures of 10 – 20 keV.

Measurements of hard x-rays made in conjunction with these experiments indicate the presence of superhot electron distributions with temperatures between 50 – 250 keV at intensities of $\sim 10^{15}$ Wcm $^{-2}$. The x-ray signal is a strongly increasing function of laser intensity in the range $5 - 9 \times 10^{14}$ Wcm $^{-2}$ and is slightly reduced by application of SSD. It appears that such superhot electrons are associated with the two-plasmon decay instability [16]. This discrepancy between the proton-inferred and x-ray-inferred hot electron temperatures is not without precedence. Tan et al. [1] found that these two types of measurement generally agreed for temperatures below 10 keV but disagreed for higher temperatures, with the x-ray inferred values being a factor of approximately 3 times greater. One possible reason for this discrepancy is that the hot-electron temperature is evolving over the duration of the pulse and the x-ray and proton methods are sensitive to different periods of this time evolution.

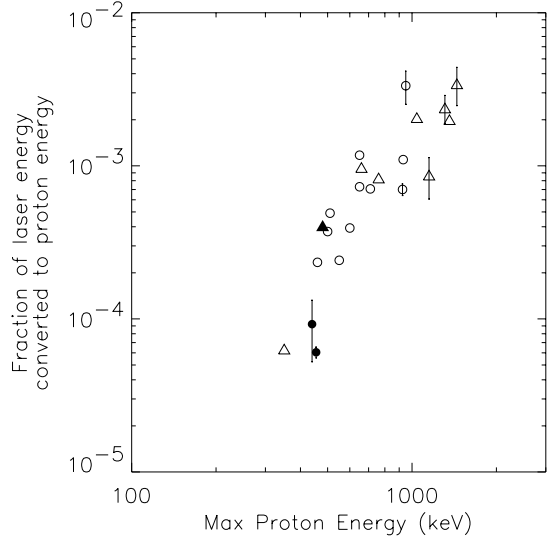


FIG. 4. Fraction of incident laser energy converted to fast protons with energies greater than 0.2 MeV plotted as a function of the endpoint energy. Plotting symbols are as in Fig. 2. Vertical bars on some data points represent the differences between the two spectrometers.

In particular, the ion acceleration is greatest early in the laser pulse when the highest ion densities give rise to the highest space-charge fields [7]. This implies that the proton spectra would weight more heavily the hot electron temperatures existing at early time periods. Understanding the origin of this temperature discrepancy may allow the two types of measurement to be used in a complementary fashion to understand the complex hot-electron distribution.

In Fig. 4, the fraction of laser energy converted to fast protons with energies greater than 200 keV is plotted versus spectral endpoint. At intensities of $\sim 10^{15}$ Wcm $^{-2}$, corresponding to an endpoint of ~ 1 MeV, the total energy carried by the fast protons is $\sim 10^{-3}$ of the laser energy, similar to the total energy of the superhot electrons inferred from x-ray data. Plastic targets, which usually produce higher maximum proton energies than glass targets irradiated at the same laser intensity, have correspondingly higher total ion energies. To within the scatter of the data, protons from the 0.4 ns shots have approximately the same fractional energy as those from the 1 ns shots. This correlation between the energy fraction and the maximum energy, regardless of target material or pulse length, indicates that the maximum proton energy can be used as a rough measure of the total energy in the fast protons. It is noteworthy that, on previous single-beam experiments [6] at higher intensities of $I\lambda^2 \sim 10^{17}$ Wcm $^{-2}$ where the maximum proton energy was also close to 1 MeV, the fraction of laser energy carried by the fast ion was also $\sim 10^{-3}$.

Also shown in Fig. 1 is a spectrum with oscillations,

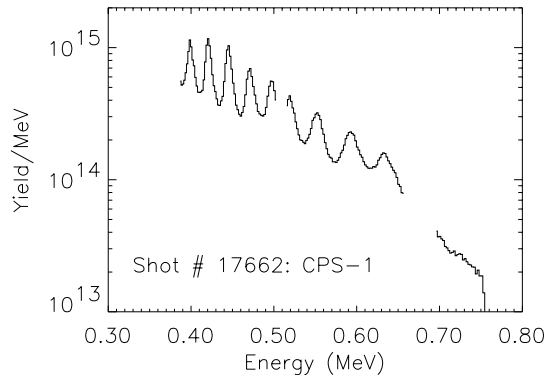


FIG. 5. Occasionally, the proton spectra exhibit discrete, regularly-spaced lines whose spacing increases with energy. These lines are super-imposed upon the exponential-like background.

features that are not repeatable from one shot to the next, and not necessarily observed on both spectrometers. Occasionally, the oscillations take the form of intense lines, as shown in Fig. 5, though it is unclear at this stage what specific conditions give rise to them. The spacing between adjacent lines increases towards higher energies, a characteristic that is common to all such line spectra. For a given laser intensity, spectra with or without lines do not show any significant difference in maximum energy.

Such strong spectral lines have not been observed before and, to the best of our knowledge, are not predicted by existing theories. One possible interpretation of these features is in terms of ion acoustic waves. A simple analysis shows that the increase in line spacing is characteristic of the behavior of ion acoustic waves in an expanding plasma. To see this, consider a plasma moving with background velocity V . An ion acoustic wave traveling in the same direction as V has a velocity $u + V$, where u is the wave velocity in the reference frame of the moving plasma. For an expanding plasma, V increases with distance in the direction of the expansion which means that the velocity of successive density peaks in the ion wave will also increase with distance in the expansion direction, producing peaks at different velocities. These peaks will be super-imposed on the exponential background spectrum as observed in Fig. 5. Using once again the isothermal, self-similar expansion model, where the plasma velocity at a given time is proportional to position, it can be shown that the difference in velocity, ΔV , between successive peaks is given approximately by $\Delta V = 2\pi(u + V)/\omega t$ where ω is the wave frequency, and t is the expansion time. Should ωt be constant over this velocity range, ΔV would be proportional to V . For the lines in Fig. 5, a plot of ΔV versus V , shown in Fig. 6, is well approximated by a straight line. Further studies will be necessary to understand the origin of these

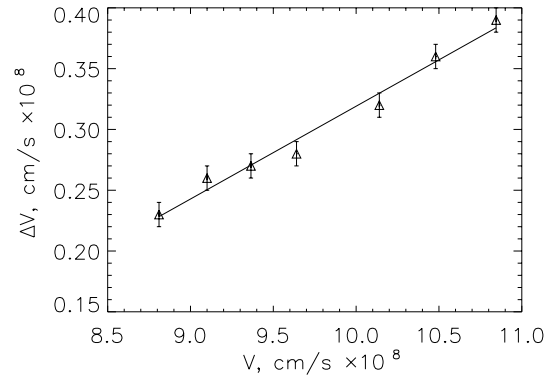


FIG. 6. A plot of the velocity difference, ΔV , between adjacent lines in Fig. 5 versus their average velocity, V . The observed linear relationship is expected if the lines are treated as the density peaks of an ion acoustic wave in the expanding plasma.

waves. Perhaps they are produced by stimulated Brillouin scattering, known to occur only at low levels on OMEGA [17], or by vibrations in the near-solid plasma before expansion.

In summary, fast protons with $\gtrsim 1$ MeV energies are produced on targets irradiated by the OMEGA, 60-beam laser system – energies more than 5 times greater than previously observed on single-beam experiments at the same $I\lambda^2$. The total energy in fast protons above 200 keV is $\sim 10^{-3}$ of the laser energy. Hot electron temperatures inferred from the proton spectra are approximately 10 – 20 keV, giving a ratio of maximum proton energy to hot electron temperature close to that observed previously. X-ray measurements indicate the presence of a 50 – 250 keV electron distribution also carrying $\sim 10^{-3}$ of the laser energy. The difference between the proton and x-ray inferred hot electron temperatures may indicate that these techniques are complementary ways of examining the hot electron distribution. Particularly striking is the new observation of intense spectral lines which may be associated with ion acoustic waves in the expanding plasma. The enhanced ion energies and appearance of discrete, spectral lines may be of interest for future ion-acceleration schemes using high-intensity lasers.

We are indebted to the OMEGA operations group for their expert help. This work was supported in part by the U.S. Dept. of Energy Contract Number DE-FG03-99SF21782, LLE sub-contract number PO410025G, LLNL sub-contract number B313975, and the U.S. Dept. of Energy Office of Inertial Confinement Fusion under Cooperative Agreement No. DE-FC03-92SF19460.

- [1] T. H. Tan, G. H. McCall, A. H. Williams, Phys. Fluids **27**, 296 (1984)
- [2] F. N. Beg et al., Phys. Plasmas **4**, 447 (1997)
- [3] S. J. Gitomer et al., Phys. Fluids **29**, 2679 (1986)
- [4] F. Begay, D. W. Forslund, Phys. Fluids **25**, 1675 (1982)
- [5] R. Decoste, B. H. Ripin, Phys. Rev. Lett. **40**, 34 (1978)
- [6] A. P. Fews et al., Phys. Rev. Lett. **73**, 1801 (1994)
- [7] J. E. Crow, P. L. Auer, J. E. Allen, J. Plasma Phys. **14**, 65 (1975)
- [8] L. M. Wickens, J. E. Allen, P. T. Rumsby, Phys. Rev. Lett. **41**, 243 (1978)
- [9] Y. Kishimoto et al., Phys. Fluids **26**, 2308 (1983)
- [10] W. Friedhorsky et al., Phys. Rev. Lett. **47**, 1661 (1981)
- [11] C. Chan et al., Phys. Fluids **27** 266 (1984)
- [12] T. R. Boehly et al., Opt. Comm., **133**, 495 (1997)
- [13] S. Skupsky, R. S. Craxton, Phys. Plasmas **6**, 2157 (1999)
- [14] D. G. Hicks et al., Rev. Sci. Instrum. **68**, 589 (1997)
- [15] D. G. Hicks, Ph.D. Thesis, Massachusetts Institute of Technology (1999)
- [16] C. Stöckl, private communication, Nov. 1999
- [17] S. P. Regan et al., Phys. Plasmas **6**, 2072 (1999)